Water Confined in Cement Pastes as a Probe of Cement Microstructure Evolution

ARTICLE *in* THE JOURNAL OF PHYSICAL CHEMISTRY B · APRIL 2009

Impact Factor: 3.3 · DOI: 10.1021/jp808754t · Source: PubMed

4 AUTHORS, INCLUDING:

Francesca Ridi
University of Florence
40 PUBLICATIONS **498** CITATIONS
SEE PROFILE

Emiliano Fratini
University of Florence
123 PUBLICATIONS **2,371** CITATIONS
SEE PROFILE

Piero Baglioni
University of Florence
448 PUBLICATIONS **7,990** CITATIONS
SEE PROFILE

THE JOURNAL OF PHYSICAL CHEMISTRY B

Article

Water Confined in Cement Pastes as a Probe of Cement Microstructure Evolution

Francesca Ridi, Paola Luciani, Emiliano Fratini, and Piero Baglioni

J. Phys. Chem. B, **2009**, 113 (10), 3080-3087• DOI: 10.1021/jp808754t • Publication Date (Web): 16 February 2009

Water Confined in Cement Pastes as a Probe of Cement Microstructure Evolution

Francesca Ridi, Paola Luciani, Emiliano Fratini, and Piero Baglioni*

Department of Chemistry and CSGI, University of Florence, via della Lastruccia 3-Sesto Fiorentino, I-50019 Florence, Italy

Received: October 3, 2008; Revised Manuscript Received: January 11, 2009

The properties of the water confined in a hydrating white cement paste have been investigated using low-temperature differential scanning calorimetry (LT-DSC) and low-temperature near infrared spectroscopy (LT-NIR). LT-DSC thermograms show, upon cooling, several exothermic peaks in the temperature range −10 to −42 °C, whose position and area depend on the hydration process, as a consequence of the cement microstructure evolution. The peaks have been interpreted in terms of Jennings' Colloidal Model-II for the hydrated calcium silicate (C−S−H) microstructure. Thermograms from samples aged up to two months from the preparation show an exothermic peak at −42 °C, typical of water confined in small gel pores (SGP). The LT-NIR results show that, at the beginning of the hydration process, water crystallizes as hexagonal ice and becomes amorphous as the setting process evolves. Both calorimetric and spectroscopic findings indicate that the water confined into the SGP porosity of the C−S−H phase (with dimension 1−3 nm) has properties very similar to those previously described for the interfacial water in zeolites, Vycor, and proteins. In particular, this confined water experiences a liquid−liquid crossover at −42 °C, passing from a high-density to a low-density liquid (HDL−LDL crossover).

Introduction

The dynamic and structural properties of water in confined geometry have been the subject of considerable interest for many years. The confinement affects the physical and chemical characteristics of this unique liquid with relevant implications in several different fields of chemical (catalysis, chemical absorption, chromatography), biophysical sciences (protein folding and unfolding), and technological applications.[1,2]

Cement is the most widely used construction material and is a fascinating system to be studied from the point of view of the water confinement. The hydration reaction kinetics of the main constituents of cement (tricalcium silicate or C_3S and dicalcium silicate or C_2S)[3] has been extensively investigated in the past using several techniques, mainly differential scanning calorimetry (DSC), Fourier transform infrared spectroscopy (FT-IR), nuclear magnetic resonance (NMR) spectroscopy, and quasielastic neutron scattering (QENS).[4−17] As a matter of fact, cement setting leads to a porous system that evolves, during the setting process, from a percolated macroporous to a micro−nanoporous structure.[18]

In this work we investigated the properties of the water confined in hydrating cementitious pastes (white cement) during the first two-months of the setting period by using low-temperature near infrared spectroscopy (LT-NIR) and low-temperature differential scanning calorimetry (LT-DSC). The progressive confinement of the water inside the paste has been addressed. We found that near the end of the hydration kinetics the unreacted water shows an exothermic transition near −40 °C upon cooling, with a broad endothermic peak in the heating scan. The LT-NIR spectra have allowed the investigation of the physical state of this confined water during the evolution of the paste. NIR is an excellent tool to study confined water-containing systems, because it is very sensitive to small changes in the water hydrogen bonds. The Gaussian deconvolution of the 7000 cm^{-1} FT-IR band gave a detailed characterization of different O−H oscillators populations and their temperature evolution. In the younger samples, where the water is able to crystallize, the Gaussian "fingerprint" of the hexagonal ice, centered at 6080 cm^{-1}, has been evidenced upon cooling and compared to data from the literature. As the hydration reaction proceeds this feature disappears, and the spectral deconvolution of the water bands discriminated the fraction of "surface-interacting" water. In particular, we show that during the first hours of hydration the presence of the solid matrix does not affect the freezing behavior of the water phase, which crystallizes as hexagonal ice, whereas for longer hydration times (more than 8 days) water experiences important structural changes, remaining in an amorphous phase also at the lowest temperature investigated (i.e., −150 °C).

Experimental Section

Ketton white cement was obtained as a generous gift by Castle Cement, through the Nanocem Consortium.

Samples for calorimetric and spectroscopic measurements have been prepared with 0.4 water/solid ratio by mass. Roughly, 40 mg of the paste were transferred in a steel pan (diameter 7.4 mm, capacity 60 μL) and sealed with the appropriate cover equipped with an O-ring to avoid vapor leaking. Samples were equilibrated at constant temperature, 20 ± 1 °C. The fluid inside pores of hermetically closed samples was in equilibrium with a 95−97% rh (relative humidity) environment.[19] For NIR experiments, approximately 500 mg of the paste were spread on a glass slide and placed in a chamber at 95 ± 1% controlled rh, in analogy with the humidity conditions of the samples for calorimetry experiments.

Differential scanning calorimetry measurements were performed using a DSC Q1000 from TA Instruments, and the data were elaborated with the Q Series software, version 3.0.3. Each

* To whom correspondence should be addressed. Phone: +39 055 457-3033; fax: +39 055 457-3032; e-mail: piero.baglioni@unifi.it, URL: www.csgi.unifi.it.

10.1021/jp808754t CCC: $40.75
Published on Web 02/16/2009

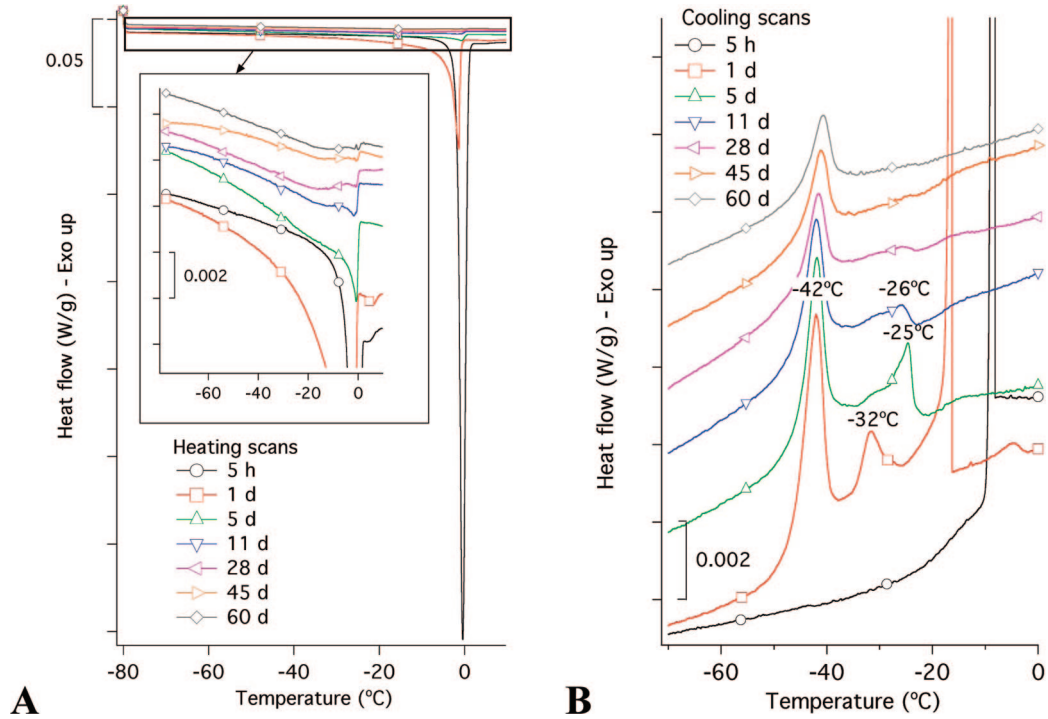

Figure 1. DSC thermograms of cement paste cured for 5 h and for 1, 5, 11, 28, 45, and 60 days. (A) Heating scans. (B) Cooling scans.[20] The reported curves are offset for clarity.

measurement was carried out with the following temperature program: equilibrate to 5 °C; cooling ramp from 5 to −80 °C at 0.5 °C/min; and heating ramp from −80 °C to +10 at 0.5 °C/min. Two different samples have been monitored throughout the curing period for each sample composition; the accuracy in the measurement of the peaks temperature was estimated to be ± 0.5 °C.

Near infrared spectra have been acquired between 10 000 and 4000 cm^{-1} with a Nexus 870-FTIR (Thermo-Nicolet) in the reflectance mode (beamsplitter: CaF_2; detector: InGaAs) with a resolution of 8 cm^{-1} and coadding 256 scans. The temperature was controlled in the range −150 °C to +20 °C, with a Linkam THMS600 stage, working under a liquid nitrogen flux. A constant dry nitrogen flux directed on the external part of the Linkam window prevented the ambient humidity from condensing on it. All the spectra have been acquired by increasing the temperature from −150 °C to 20 °C. To consider the small part of the incident light transmitted by the sample, each single beam spectrum was processed with a reference background acquired at the same temperature on a silver surface, using the Kubelka−Munk algorithm. During the acquisition of the silver backgrounds a vessel with anhydrous $CaCl_2$ was placed in the Linkam chamber, in order to eliminate any trace of humidity from the chamber itself.

Results

Differential Scanning Calorimetry. The presence of water inside the curing paste and its freeze−thaw behavior have been characterized by DSC measurements, between room temperature and −80 °C.

Figure 1 reports the thermograms for cement/water paste at 5 h and at 1, 5, 11, 28, 45, and 60 days after mixing.

All heating scans (from −80 °C to room temperature) show a single hump over the whole temperature range, as clearly evidenced in the inset of Figure 1A. On the other hand, in the corresponding cooling scans (Figure 1B) some thermal features are also evident in the low-temperature range. In particular, a characteristic peak centered at −42 °C grows after 1 day and remains until 2 months after the preparation of the paste. Other peaks, in the temperature range between −25 and −35 °C, are present and evolve during the hydration process. This progress in the LT-DSC thermograms of cement pastes has already been reported in the literature.[19,21−23] The absence of equivalent peaks in the low-temperature range of the heating part of the thermograms has been explained according to the evidence that the pore size distribution in a cement paste is unimodal;[19] since no characteristic dimensions of pores are present, the melting process occurs as a continuous release of heat from the thawing of water contained in pores with increasing dimension, producing only a hump during the overall heating process. On the contrary, when the sample is subjected to cooling, the ice front would progressively advance, penetrating the pores and producing the crystallization of the water confined in the porosity. In this case, the solidification temperature will depend on the dimension of the pores entrances, rather then on the dimensions of the pores. Hence, the characteristic freeze−thaw behavior of cement pastes, as detected by DSC, would indicate that the bulk microstructure has a unimodal pore size distribution with characteristic dimensions of the channels connecting the pores. In the recent years, Jennings, based on the huge amount of data present in the literature, formulated a clear and coherent model for the cement microstructure. The basic idea of the model is that the bulk microstructure is formed as a consequence of the packing of basic particles (globules) having peculiar shape and internal structure. The first version of the model (recently referred at as Colloidal Model-I, CM-I[24]) primarily focused on explaining how the properties of the material depend on the packing behavior of the basic globules. In that context, the influence of the globules' internal structure on the bulk properties was not explored in detail.[25]

Snyder and Bentz[19] used the CM-I model to interpret the LT-DSC obtained for the C−S−H hydrated phase. They associated

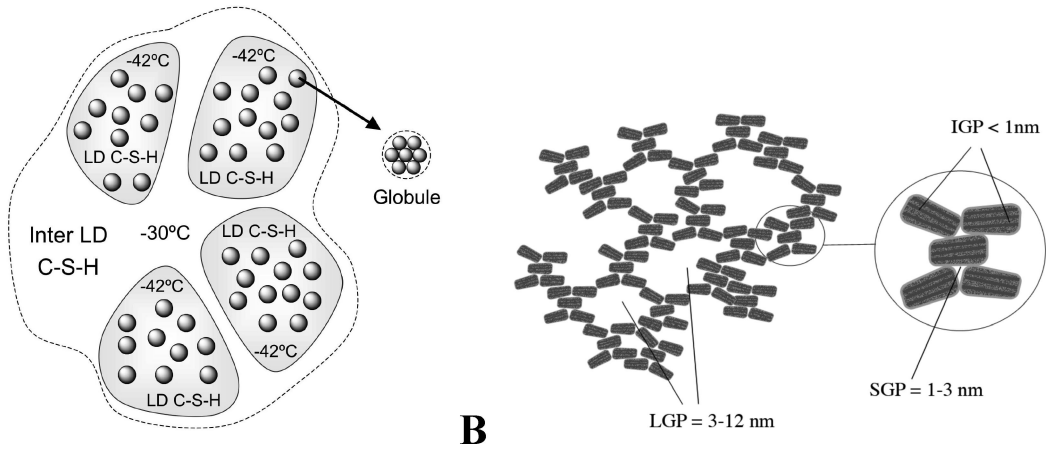

Figure 2. Schematic representation of the Jennings colloidal models for the cement microstructure. (A) Colloidal Model-I, CM-I; (B) Colloidal Model-II, CM-II.

the peaks detected in the cooling scan to "water reservoirs", that is, relatively large pores interconnected through small channels, with nanometric diameter. In the framework of the CM-I model, the peak in the region between −20 and −35 °C was assigned to water only accessible via the inter-LD pores[19,25−27] (see Figure 2A). On the other hand, the peak below −40 °C should correspond to pores inside the low-density C−S−H (LD C−S−H) (see Figure 2A), whose dimension was estimated to be around 1 nm.[19,28−31]

The CM-I model has been very recently modified and extended to take into account the smallest porosity of the C−S−H phase associated to the basic globules′ internal structure,[24] (Colloidal Model-II, CM-II). The CM-II model represents a significant upgrade in the description of cement microstructure, since it reconciles many controversial data reported in the literature. In particular, this model gives an exhaustive interpretation of the sorption isotherms experiments. According to CM-II, the microstructure of a cement paste can be schematically described as in Figure 2B: the basic globule is a disk-like object, whose thickness is around 4 nm, having a layered internal structure. The water inside the globule is located both in the interlamellar spaces and in very small cavities (intraglobular pores, IGP), with dimensions ≤1 nm. The packing of these globules produces a porous structure, where two other main pores populations can be identified: the small gel pores (SGP), with dimensions 1−3 nm; and the large gel pores (LGP), 3−12 nm in size. The inclusion of the sub-nanometric porosity in the description of the microstructure justifies most of the experimental evidence, representing a decisive step for the understanding and the control of the relationships between structure and properties.

Having this picture in mind, the LT-DSC thermograms recorded during the hydration process of the white cement/water paste can be interpreted in the light of the CM-II model, thus providing direct information on the local microstructure evolution.

After 5 h from the sample preparation, the growth of the hydrated products has not yet started, and the paste is still fluid. At this time, the corresponding DSC cooling thermogram (Figure 1B) shows only a freezing peak, centered at −10 °C, that can be attributed to the freezing of the water. In fact, the supercooling of bulk water, a well-studied phenomenon,[32] occurs randomly between −15 and −30 °C due to the lack of nucleation sites. In the presence of a solid phase, such as zeolites,[33] this temperature significantly increases due to the nucleation sites provided by the solid particles. Therefore, the peak at −10 °C recorded for the freezing of water in the hydrating paste (5 h) is in complete agreement with the values reported for water in contact with an inorganic solid phase.[33]

After one day from the mixing, three freezing peaks are evident in the cooling part of the thermogram (Figure 1B). The most intense peak is centered at −20 °C, and 2 other exothermic features occur at −42 and −32 °C, respectively, close to the values reported by Snyder and Bentz[19] for Portland cement. As a result of the increased confinement in the developing C−S−H matrix, the "bulk" water still present in the sample freezes at −20 °C, a much lower temperature than that expected in the presence of an inert solid surface. This is also validated by the increased depression of the melting peak (red curve in Figure 1A; $T_M = -1.4$ °C).

Only the peaks at lower temperature (<−25 °C) continue to be present after five days from the sample preparation, evidencing that all the unreacted water is strictly confined in the developing microstructure. The presence of two populations of confined water has been previously detected in the same white cement paste (w/c = 0.4) after a few days of hydration, by means of ^{1}H nuclear magnetic resonance relaxometry.[31] It was estimated that the dimensions of these different reservoirs are, respectively, 1.0−1.7 and ≥7 nm, thus broadly corresponding to the SGP and LGP porosities as reported in the CM-II model. No signals due to the IGP and interlamellar water were detected, probably because the associated relaxation times are too small to be detected experimentally.

Similarly, in our LT-DSC experiments two populations of constrained water are detected. The temperatures of the freezing peaks assessed via the LT-DSC cooling scans are consistent with the sizes estimated in the CM-II model for the SGP and LGP porosities, respectively. The literature reports a freezing peak around −40 °C for water confined in pores of 1−3 nm,[34,35] whereas the water confined in larger pores freezes between −20 and −35 °C.[36−38] When the confinement is more severe (≤1 nm), no freezing peak is detected, as demonstrated with synthetic nanoporous silica matrices with controlled pore sizes.[34] For this reason the water confined in the internal structure of the basic C−S−H globules cannot be detected by LT-DSC.

As the hydration reaction proceeds, all the water confined in the LGP is consumed (i.e., the peaks between −20 and −35 °C disappear), and after 1 month only the water in SGP is present in the paste.

To quantify the different populations of water in the sample ("bulk-like", LGP, and SGP) and their evolution during the hydration process, the area under each peak has been estimated. Each freezing curve was plotted as heat flow versus time, and

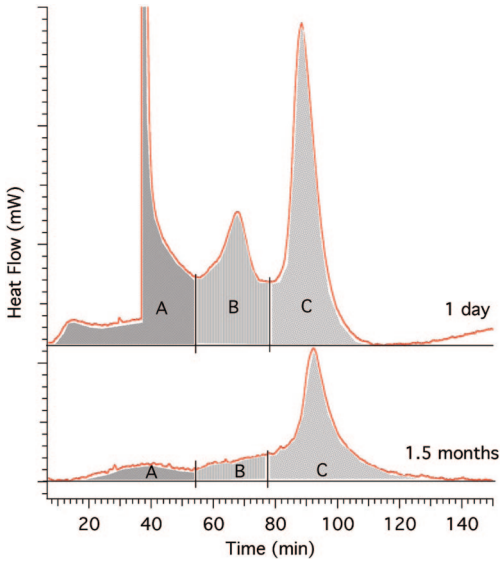

Figure 3. Cooling part of the thermograms of the cement paste cured 1 day and 1.5 months (heat flow vs time). The three integrated regions are evidenced by the letters A (bulk-like water region), B (water in LGP) and C (water in SGP).

TABLE 1: Evolution of Water Amount[a] Freezing in Regions A, B, and C

hydration time	water (%) bulk-like [b]	in LGP [c]	in SGP [d]
5 h	73.6		
1 d	19.4	3.0	5.4
5 d	0.7	2.6	6.3
11 d	0.4	1.4	5.1
1 m	0.4	0.9	3.4
1.5 m	0.6	0.7	3.2
2 m	0.2	0.6	2.8

[a] The percentages are calculated with respect to the initial amount of water added in the mix.[41] [b] Region A: water freezing from room temperature to −20 °C. [c] Region B: water freezing between −20 and −35 °C. [d] Region C: water freezing between −35 and −50 °C.

the baseline was subtracted. The area under the subtracted curve was arbitrarily divided into three regions, as shown in Figure 3: above −20 °C (bulk-like water, region A), between −20 and −35 °C (water confined in the LGP space, region B), and below −35 °C (water confined in SGP porosity, region C).

The heat of fusion is a function of the temperature.[39,40] Hansen et al.[40] calculated the heat of fusion of water confined in completely hydrated cement pastes (i.e., cured under water), between −60 and 10 °C, by the combined use of NMR and calorimetry measurements. In particular, they correlated the amount of melted ice as measured by NMR to the amount of released heat as measured by calorimetry, thus deriving a linear dependence of the heat of fusion in respect of the inverse of temperature. To calculate the water amount for regions A, B, and C under the thermograms, we used Hansen's estimation of ΔH at the mean temperature within each region, whereas when a melting peak was present, the ΔH estimated at the peak maximum temperature was used. The obtained values are reported in Table 1.

It is interesting to note that the amount of water constrained in the SGP (freezing at −42 °C) increases until 5 days from the mixing, meaning that the microstructure is strongly developing during the first week. At later times, when the bulk water has almost completely reacted, these water reservoirs start to be consumed by the hydration reaction, as shown by the decrease in the area of region C.

It is important to note that, within our experimental setup, that is, under sealed conditions, the larger pores are not completely full. As a matter of fact, the "chemical shrinkage" phenomenon reduces the internal relative humidity to 90−95%, causing the partial emptying of the larger pores. For this reason the present data have not been interpreted in terms of pore collapse or disappearing, but rather in terms of the progressive consumption of the water contained in the larger pores. The comparison of the present data with measurements on samples cured in saturated conditions is in progress, and it will be the subject of a future investigation, in order to clarify this point.

Near Infrared Spectroscopy. To investigate the nature of the water confined in the hydrated cement matrix, we performed LT-NIR spectroscopy experiments during the hydration process.

In a previous work[42] we applied for the first time the NIR spectroscopy to the study of tricalcium silicate hydration, and we showed that this technique is particularly suitable for the investigation of systems containing confined water. The infrared absorption is very sensitive to the changes in hydrogen bond strength, and for this reason it can address the water populations differently confined in a solid matrix and interacting with a surface.[42,43] In this work we further improve the NIR investigation of cementitious pastes. The evolution of the NIR bands has been monitored in the temperature range between −150 and +20 °C, at different hydration times. The 7000 cm^{-1} band (first O−H stretching overtone) of each spectrum has been fitted in terms of Gaussian components, according to the following equation:

$$F(\lambda) = y_0 + \sum_{j=1}^{N} \frac{y_j}{\sigma_j\sqrt{2\pi}} \exp\left[\frac{(\lambda - \lambda_j)^2}{2\sigma_j^2}\right]$$

where y_j, λ_j, and σ_j are the weight, peak wavenumber and width of the jth Gaussian component. The number of Gaussian components used for the band reconstruction can vary according to the hydration time and temperature. The simplest case corresponds to the fresh sample (up to 3 h), at room temperature, where only three components are necessary to describe the vibrational modes of the O−H oscillators associated with the unreacted water (Figure 4A). As reported in the literature,[42,44] the component at higher wavenumber, usually named α, accounts for the "surface-interacting" water, whereas the other two components (β and γ) account for the bulk-like water molecules. As the reaction proceeds, an extra component must be added (ϵ) in order to take into account the first overtone (7089 cm^{-1}) coming from the stretching mode of the O−H oscillators belonging to the Portlandite, $Ca(OH)_2$, that is produced as a byproduct of the cement curing (Figure 4B). Finally, a fifth component (η) must be included (Figure 4C) in order to describe the hexagonal ice band (where present in the low T cases).

The temperature dependence of the NIR bands of pure hexagonal ice[46−48] has been described in great detail in the literature. In particular, Grundy and Schmitt provided a complete description of the ice NIR bands as a function of temperature, which is very important for geophysical research, particularly for the determination of the temperature of icy regions in remote planets.[47] Grundy and Schmitt's ice description can be used to explain our results between −150 and +20 °C in the case of 3 h, 1 day, 8 days, and 1 month old cement pastes.

Figure 5 shows the spectra registered for the 3 h-old sample. As already mentioned, the fitting of the curves registered at

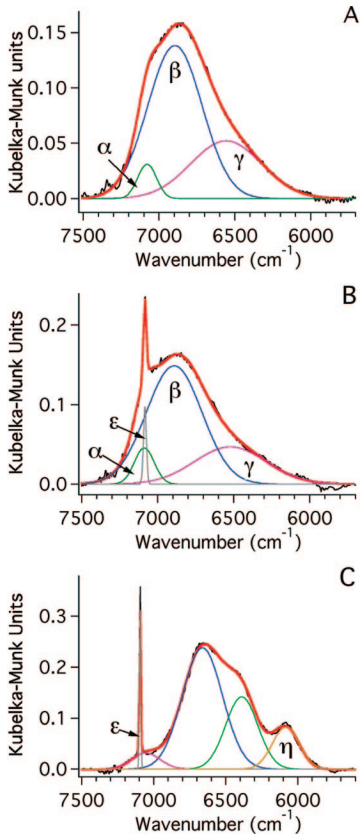

Figure 4. Spectral deconvolution of the 7000 cm^{-1} part of the NIR spectra. (A) Spectrum registered at 20 °C for 3 h-cured paste; (B) spectrum registered at 20 °C for 1 day-cured paste; (C) spectrum registered at −150 °C on the 1 day-cured paste.[45]

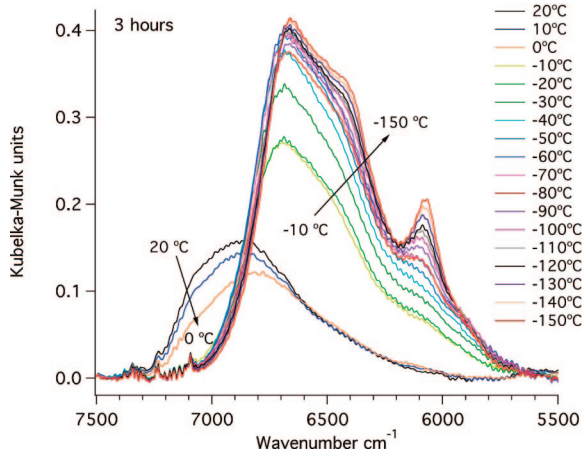

Figure 5. NIR spectra acquired from −150 to +20 °C on cement paste cured for 3 h.

higher temperature (20, 10, and 0 °C) on the 3 h sample was obtained with three Gaussian components, (α, β, and γ) to account for the water phase.[42] The temperature decrease results in a profound modification of the NIR band shapes: as expected for liquid water, the NIR absorption around 7000 cm^{-1} moves toward lower wavenumbers.[44,46] In particular, a net red shift of the whole band occurs in correspondence to the freezing process, and the ice formation manifests itself with the growth of a new band centered near 6080 cm^{-1}. To fully describe the band shape, the addition of a further Gaussian component (named η) was necessary below −10 °C. This spectral feature centered around 6080 cm^{-1} is commonly recognized as a fingerprint of hexagonal

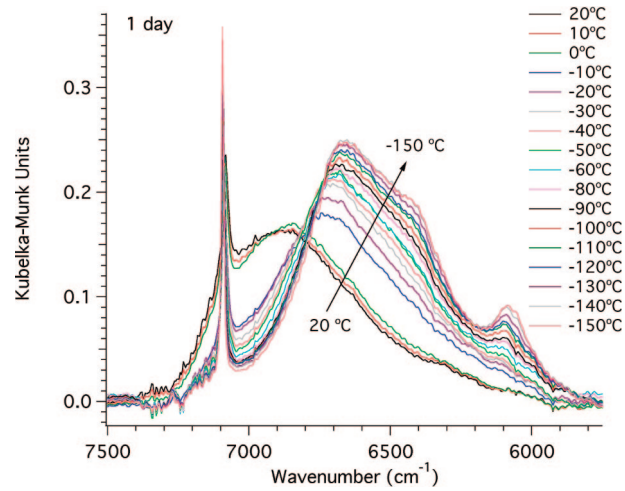

Figure 6. NIR spectra acquired from −150 to +20 °C on cement paste cured for 1 day.

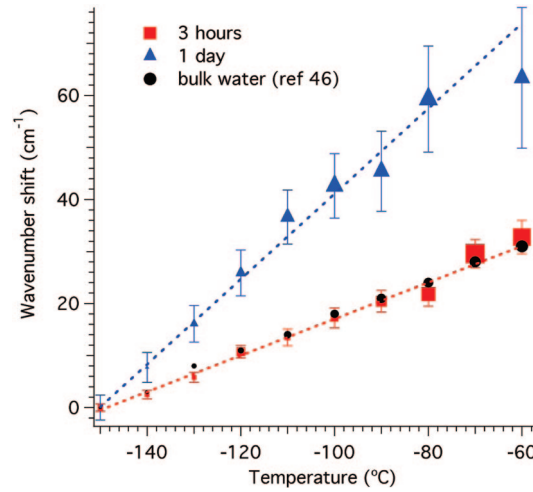

Figure 7. Wavenumber shift vs temperature for the η Gaussian relative to the −150 °C value as obtained from the deconvolutions of the 3 h- and 1 day-old samples. The size of the dots varies according to the amplitude of the Gaussian. The data for bulk water taken from ref 46 are reported as a comparison (black dots).

ice, even if no theoretical or experimental attribution of these ice vibrational modes has yet been published.[46−48]

After 1 day (see Figure 6) an additional Gaussian (ϵ) was needed because of the presence of calcium hydroxide, as already mentioned. Except for the presence of this additional absorption due to calcium hydroxide, the same considerations already drawn for the 3 h-old sample hold.

Figure 7 describes the temperature evolution of the amplitude and wavenumber shift of the η Gaussian component, relative to hexagonal ice in the 3 h- and the 1 day-old samples. The data obtained by Grundy et al.[46] for a pure hexagonal ice phase is included for comparison. In all cases, the wavenumber decreases linearly with temperature, and the line shape becomes narrower (i.e., the amplitude decreases, while its intensity increases). This effect can be explained by an increase in the lattice structural order, which maximizes the hydrogen bonds (distances and angles) and decreases the covalent O−H bond strength,[44] imposed by the temperature lowering. The 3 h-old sample mimics the behavior of a pure hexagonal ice phase, in agreement with published data.[46] On the other hand, after 1 day from the mixing, the slope $\Delta\nu/\Delta T$ doubles (i.e., the temperature change produces a greater shift), indicating that a less-ordered ice phase crystallizes inside cement pastes as the hydration

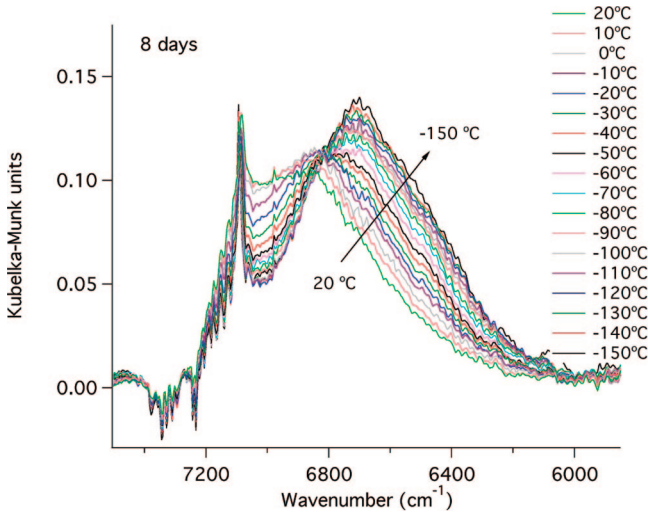

Figure 8. NIR spectra acquired from −150 to +20 °C on cement paste cured for 8 days.

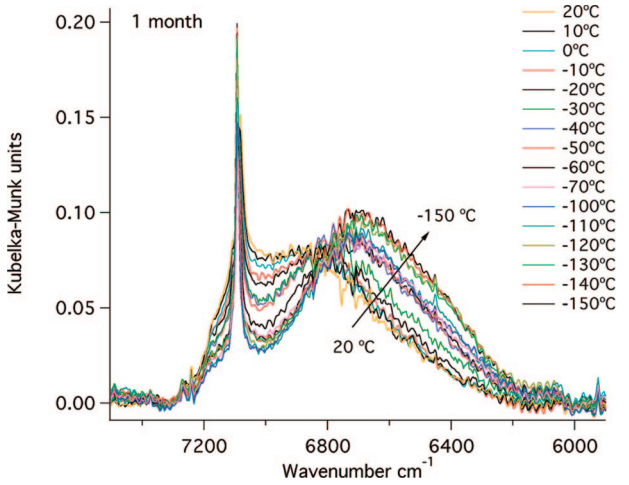

Figure 9. NIR spectra acquired from −150 to +20 °C on cement paste cured for 1 month.

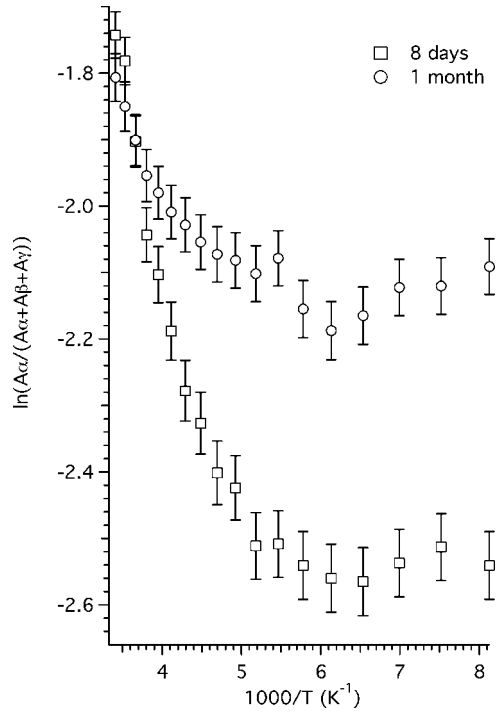

Figure 10. Van't Hoff plots of the $A_\alpha/(A_\alpha + A_\beta + A_\gamma)$ ratio for the samples cured for 8 days and 1 month.

TABLE 2: Evolution of the Water Confined in SGP with Respect to the Total Freezing in the Sample at Each Hydration Time

hydration time	water in SGP (% ±5%)
5 h	
1 day	19
5 days	65
11 days	74
1 month	72
1.5 months	70
2 months	77

reaction proceeds and the developing C−S−H phase modifies the hydrogen bonded network.

The spectra registered after 8 days and 1 month are reported in Figures 8 and 9, respectively. Two main differences can be noted with respect to younger samples: the shift to higher wavenumbers is less marked, and the ice fingerprint (i.e., η band) is no longer present. This is a strong indication that, due to the confinement effect of the developing solid matrix, the constrained water in the 8 days-old sample does not crystallize anymore as hexagonal ice. According to the literature,[48] the 7000 cm^{-1} band-shape and its evolution with temperature after 8 days in the cement paste indicate that the water is in an amorphous state.

The 7000 cm^{-1} band of the spectra at 8 days and 1 month was very well fitted with four Gaussian components: α, β, γ, and ϵ. As described in the literature, and extensively discussed by us in a previous work,[42] among the three Gaussian curves accounting for the water vibrational modes in the NIR region, the α Gaussian, at higher wavenumbers, is originated by the "weakly hydrogen-bonded" class of molecules. For 3 h- and 1 day-old samples, as for bulk water, the fraction of weakly hydrogen-bonded molecules disappears as the temperature reaches the freezing point. For supercooled water, this population tends to zero as the temperature approaches the critical divergence (about $T = 228$ K).[43,49,50] When the dynamic of the water molecules is strongly coupled to a surface, as in the case of dry silica hydrogel,[43] the α Gaussian does not show this critical divergence. The same behavior occurs in our system. Figure 10 reports the Van't Hoff plot of the quantity $A_\alpha/(A_\alpha + A_\beta + A_\gamma)$ (A_x being the areas of the Gaussian components) for the cement paste cured 8 days and 1 month. Both curves reach a plateau for temperatures lower than −80 °C. The plateau indicates that after 8 days roughly the 8% of the unreacted water is surface-interacting, whereas after 1 month this fraction increases up to about 12%.

Discussion

The LT-DSC thermograms show that after 5 days of curing most of the water is confined in the SGP porosity, that is, in the 1−3 nm sized spaces between the packed basic globules of C−S−H. The evidence in Table 2 shows that after 11 days the water confined in SGP is more than 70%. This water exhibits a well-defined transition upon cooling, with a large hysteresis in the heating scan. On the other hand, the LT-NIR experiments show that this water does not crystallize as hexagonal ice.

Differently from other simple molecular liquids, water is known to present peculiar properties when the temperature is decreased. In particular, the main thermodynamic response functions (derivatives of the state functions with respect of the

temperature) of the supercooled water, such as isobaric heat capacity, isothermal compressibility, and thermal expansion coefficient, show a divergent behavior as temperature diminishes. The literature reports some possible hypothesis in order to account for this behavior. One of the most reliable explanation suggests that the supercooling anomalies are caused by the existence of a low-temperature critical point; molecular dynamics calculations[51,52] and the extrapolation of the values obtained in the accessible range of temperature[2,53,54] locate this point around −45 °C. This critical point represents a crossover between a fragile behavior (at higher temperature) and a strong behavior (at lower temperature). These two distinct supercooled liquid phases are also called high-density liquid (HDL, fragile) and low-density liquid (LDL, strong). Experimental evidence of this liquid−liquid crossover have been already described for interfacial water in several different systems: zeolites,[35] Vycor,[55] MCM41,[34] and lysozyme.[56] For both zeolites and Vycor at low hydration levels (corresponding to a complete monolayer on the pore surface), the LT-DSC thermograms present an exothermic peak, upon cooling, in the region around −40 °C, with a related broad endothermic hump in the heating scan. On the other hand, in the case of Vycor confined water, Zanotti et al.[55] did not evidence any typical ice diffraction peaks by means of neutron diffraction experiment, demonstrating that water does not crystallize in this system.

In the present work we show that the water confined in the SGP—pores having a size from 1 to 3 nm—present in a cured cement paste shows the same calorimetric behavior of the interfacial water present in zeolites, Vycor, and proteins, that is, a sharp exothermic transition at −42 °C, when the system is subjected to cooling, and a correspondent broad endothermic peak in the heating part. Concurrently, the LT-NIR spectroscopy does not evidence any crystallization associated with the calorimetric transition, even decreasing the temperature down to −150 °C. This behavior confirms that the water confined in the C−S−H SGP spaces of a hydrating cement paste presents the same HD-LD liquid−liquid crossover, previously described for different systems (i.e., zeolites, Vycor, and proteins). Very recently, a quasi-elastic neutron scattering (QENS) study has been performed on the same white cement paste (w/c = 0.4) after 8 days of curing, in order to have a deeper evidence of the liquid−liquid crossover.[57] In particular, the average relaxation time accounting for the hydrogenated mobile species (i.e., confined water) as extracted by QENS shows clear evidence of a super-Arrhenius (nonlinear behavior) to Arrhenius (linear behavior) crossover if plotted as a function of the inverse temperature. This dynamic feature, usually referred to as fragile to strong crossover, is present at −42 ± 5 °C and marks the change in structure from a HDL to a LDL phase upon cooling. If taken together with the LT-DSC and LT-NIR evidence, it strongly reinforces the conclusion that the water constrained in the SGP in a cured cement paste undergoes a liquid−liquid crossover.

Conclusions

In this paper, we study the properties of the water confined in a hydrating cement paste by means of LT-DSC and LT-NIR. The LT-DSC thermograms evidence several exothermic features in the temperature range −10 to −42 °C, when the hydrating paste is subjected to cooling. These peaks evolve during the hydration process and have been interpreted in terms of Jennings′ Colloidal Model-II for the cement microstructure. The exothermic peak at −42 °C persists up to two months from the sample preparation and can be attributed to the water confined in the SGP. The LT-NIR technique shows that, at the end of the hydration process, the unreacted water is strictly confined and no more subjected to crystallization. As a matter of fact, the NIR spectra temperature evolution does not evidence any hexagonal ice fingerprint, rather indicating that the water is in an amorphous phase. The experimental calorimetric and spectroscopic evidence, in agreement with previous studies on interfacial water in different confining matrices and with recent findings in white cement pastes,[57] indicate that the water constrained into the C−S−H SGP porosity (1−3 nm) experiences a liquid−liquid crossover at −42 °C, passing from high-density to low-density liquid upon cooling.

Acknowledgment. Financial support from Ministero dell′Istruzione, Università e della Ricerca Scientifica (MIUR, grant PRIN-2006) and Consorzio Interuniversitario per lo Sviluppo dei Sistemi a Grande Interfase, CSGI, is gratefully acknowledged. Authors thank the Referees, for their positive and constructive comments that greatly improved the final version of this paper.

References and Notes

(1) Wang, J.; Zhu, Y.; Zhou, J.; Lu, X. H. *Phys. Chem. Chem. Phys.* **2004**, *6*, 829–835.
(2) Mallamace, F.; Chen, S. H.; Broccio, M.; Corsaro, C.; Crupi, V.; Majolino, D.; Venuti, V.; Baglioni, P.; Fratini, E.; Vannucci, C.; Stanley, H. E. *J. Chem. Phys.* **2007**, *127*, 045104.
(3) We adopt the well-accepted cement chemistry notation where: C = C_3S, S = SiO_2 and H = H_2O. Within this notation the tricalcium silicate is abbreviated as CaO, dicalcium silicate is C_2S, and the calcium silicate hydrated phase becomes C−S−H.
(4) FitzGerald, S. A.; Neumann, D. A.; Rush, J. J.; Bentz, D. P.; Livingston, R. A. *Chem. Mater.* **1998**, *10*, 397–402.
(5) Fratini, E.; Chen, S. H.; Baglioni, P.; Bellissent-Funel, M. C. *Phys. Rev. E* **2001**, *64*, 1–4.
(6) Baglioni, P.; Fratini, E.; Chen, S. H. *Appl. Phys. A: Mater. Sci. Process.* **2002**, *74*, S1178−S1181.
(7) Faraone, A.; Chen, S. H.; Fratini, E.; Baglioni, P.; Liu, L.; Brown, C. *Phys. Rev. E* **2002**, *65*, 040501−040504.
(8) Fratini, E.; Chen, S. H.; Baglioni, P.; Bellissent-Funel, M. C. *J. Phys. Chem. B* **2002**, *106*, 158–166.
(9) Fratini, E.; Chen, S. H.; Baglioni, P.; Cook, J. C.; Copley, J. R. D. *Phys. Rev. E* **2002**, *65*, 010201.
(10) Fratini, E.; Faraone, A.; Baglioni, P.; Bellissent-Funel, M. C.; Chen, S. H. *Physica A* **2002**, *304* (1−2), 1–10.
(11) Damasceni, A.; Dei, L.; Fratini, E.; Ridi, F.; Chen, S. H.; Baglioni, P. *J. Phys. Chem. B* **2002**, *106*, 11572–11578.
(12) Fratini, E.; Chen, S. H.; Baglioni, P. *J. Phys. Chem. B* **2003**, *107*, 10057–10062.
(13) Ridi, F.; Dei, L.; Fratini, E.; Chen, S. H.; Baglioni, P. *J. Phys. Chem. B* **2003**, *107*, 1056–1061.
(14) Faraone, A.; Fratini, E.; Baglioni, P.; Chen, S. H. *J. Chem. Phys.* **2004**, *121*, 3212–3220.
(15) Alesiani, M.; Capuani, S.; Giorgi, R.; Maraviglia, B.; Pirazzoli, I.; Ridi, F.; Baglioni, P. *J. Phys. Chem. B* **2004**, *108*, 4869–4874.
(16) Ridi, F.; Fratini, E.; Mannelli, F.; Baglioni, P. *J. Phys. Chem. B* **2005**, *109*, 14727–14734.
(17) Fratini, E.; Ridi, F.; Chen, S. H.; Baglioni, P. *J. Phys.: Condens. Matter* **2006**, *18*, S2467−S2483.
(18) Taylor, H. F. W. *Cement Chemistry*, 2nd ed.; Thomas Telford: London, 1997.
(19) Snyder, K. A.; Bentz, D. P. *Cem. Concr. Res.* **2004**, *34*, 2045–2056.
(20) The very small feature present at −5 °C in the cooling thermogram registered after 1 day is probably due to the well-known bleeding phenomenon.
(21) Bager, D. H.; Sellevold, E. J. *Cem. Concr. Res.* **1986**, *16*, 709–720.
(22) Bager, D. H.; Sellevold, E. J. *Cem. Concr. Res.* **1986**, *16*, 835–844.
(23) Bager, D. H.; Sellevold, E. J. *Cem. Concr. Res.* **1987**, *17*, 1–11.
(24) Jennings, H. M. *Cem. Concr. Res.* **2008**, *38*, 275–289.
(25) Jennings, H. M. *Cem. Concr. Res.* **2000**, *30*, 101–116.
(26) Tennis, P. D.; Jennings, H. M. *Cem. Concr. Res.* **2000**, *30*, 855–863.
(27) Thomas, J.; Jennings, H. M. *Cem. Concr. Res.* **2006**, *36*, 30–38.
(28) Jennings, H. M.; Tennis, P. D. *J. Am. Ceram. Soc.* **1994**, *77*, 3161–3172.

(29) Valckenborg, R. M. E.; Pel, L.; Kopinga, K. *J. Phys., D, Appl. Phys.* **2002**, *35*, 249–256.
(30) Pratt, P. L.; Jennings, H. M. *Annu. Rev. Mater. Sci.* **1981**, *11*, 123.
(31) Monteilhet, L.; Korb, J. P.; Mitchell, J.; McDonald, P. *J. Phys. Rev. E* **2006**, *74*, 061401−061409.
(32) Mason, B. J. *Adv. Phys.* **1958**, *7*, 221–234.
(33) Janssen, A. H.; Talsma, H.; van Steenbergen, M. J.; de Jong, K. P. *Langmuir* **2004**, *20*, 41–45.
(34) Liu, L.; Chen, S. H.; Faraone, A.; Yen, C. W.; Mou, C. Y.; Kolesnikov, A. I.; Mamontov, E.; Leao, J. *J. Phys.: Condens. Matter* **2006**, *18*, S2261−S2284.
(35) Takamuku, T.; Yamagami, M.; Wakita, H.; Masuda, Y.; Yamaguchi, T. *J. Phys. Chem. B* **1997**, *101*, 5730–5739.
(36) Landry, M. R. *Thermochim. Acta* **2005**, *433*, 27–50.
(37) Iza, M.; Woerly, S.; Danumah, C.; Kaliaguine, S.; Bousmina, M. *Polymer* **2000**, *41*, 5885–5893.
(38) Ishikiriyama, K.; Todoki, M.; Motomura, K. *J. Colloid Interface Sci.* **1995**, *171*, 92–102.
(39) Defay, R.; Prigogine, I.; Bellemans, A.; Everett, D. H. *Surface Tension and Adsorption*, 1st ed.; Longmans: London, 1966.
(40) Hansen, E. W.; Gran, H. C.; Sellevold, E. J. *J. Phys. Chem. B* **1997**, *101*, 7027–7032.
(41) The standard deviation on each value is about ±1%, so values below 1% are meaningless and can be considered zero.
(42) Ridi, F.; Fratini, E.; Milani, S.; Baglioni, P. *J. Phys. Chem. B* **2006**, *110*, 16326–16331.
(43) Cupane, A.; Levantino, M.; Santangelo, M. G. *J. Phys. Chem. B* **2002**, *106*, 11323–11328.
(44) Angell, C. A.; Rodgers, V. *J. Chem. Phys.* **1984**, *80*, 6245–6252.
(45) It is important to note that the hexagonal ice spectrum (C) significantly differs from that of the liquid water, especially at low temperature. For this reason, apart from the ϵ curve, due to the $Ca(OH)_2$, the wavenumbers of the Gaussian curves describing it do not correspond to those of the α, β, and γ curves.
(46) Grundy, W. M.; Schmitt, B. *J. Geophys. Res.* **1998**, *103*, 25809–25822.
(47) Grundy, W. M.; Buie, M. W.; Stansberry, J. A.; Spencer, J. R. *Icarus* **1999**, *142*, 536–549.
(48) Mastrapa, R. M. E.; Brown, R. H. *Icarus* **2006**, *183*, 207–214.
(49) Speedy, R. J.; Angell, C. A. *J. Chem. Phys.* **1976**, *65*, 851.
(50) Angell, C. A. *Annu. Rev. Phys. Chem.* **1983**, *34*, 593.
(51) Poole, P. H.; Sciortino, F.; Essmann, U.; Stanley, H. E. *Nature* **1992**, *360*, 324–328.
(52) Poole, P. H.; Sciortino, F.; Grande, T.; Stanley, H. E.; Angell, C. A. *Phys. Rev. Lett.* **1994**, *73*, 1632–1635.
(53) Liu, L.; Chen, S. H.; Faraone, A.; Yen, C. W.; Mou, C. Y. *Phys. Rev. Lett.* **2005**, *95*, 117802.
(54) Mallamace, F.; Broccio, M.; Corsaro, C.; Faraone, A.; Wanderlingh, U.; Liu, L.; Mou, C. Y.; Chen, S. H. *J. Chem. Phys.* **2006**, *124*, 161102.
(55) Zanotti, J.-M.; Bellissent-Funel, M. C.; Chen, S. H. *Europhys. Lett.* **2005**, *71*, 91–97.
(56) Chen, S. H.; Liu, L.; Fratini, E.; Baglioni, P.; Faraone, A.; Mamontov, E. *PNAS* **2006**, *103*, 9012–9016.
(57) Zhang, Y.; Lagi, M.; Ridi, F.; Fratini, E.; Baglioni, P.; Mamontov, E.; Chen, S. H. *J. Phys.: Condens. Matter* **2008**, *20*, 502101–502106.

JP808754T